

USEV: Universal Speaker Extraction with Visual Cue

Zexu Pan, Meng Ge, and Haizhou Li, *Fellow, IEEE*

Abstract—A speaker extraction algorithm seeks to extract the target speaker’s voice from a multi-talker speech mixture. An auxiliary reference, such as a video recording or a pre-recorded speech, is usually used as a cue to form a top-down auditory attention. The prior studies are focused mostly on speaker extraction from a multi-talker speech mixture with highly overlapped speakers. However, a multi-talker speech mixture is often sparsely overlapped, furthermore, the target speaker could even be absent sometimes. In this paper, we propose a universal speaker extraction network that works for all multi-talker scenarios, where the target speaker can be either absent or present. When the target speaker is present, the network performs over a wide range of target-interference speaker overlapping ratios, from 0% to 100%. The speech in such universal multi-talker scenarios is generally described as sparsely overlapped speech. We advocate that a visual cue, i.e. lips movement, is more informative to serve as the auxiliary reference than an audio cue, i.e. pre-recorded speech. In addition, we propose a scenario-aware differentiated loss function for network training. The experimental results show that our proposed network outperforms various competitive baselines in disentangling sparsely overlapped speech in terms of signal fidelity and perceptual evaluations.

Index Terms—Multi-modal, target speaker extraction, time-domain, sparsely overlapped speech, scenario-aware differentiated loss.

I. INTRODUCTION

HUMAN has the inherent ability to selectively listen to a speaker in a multi-talker scenario, also known as the selective auditory attention [1] in *cocktail party* problem [2]. Ever since the problem is formulated, the quest for an engineering solution has never stopped. Selective auditory attention is non-trivial, but highly demanded in real-world applications such as hearing aids [3], speaker verification [4], and speech recognition [5].

This research is supported by Programmatic Grant No. A18A2b0046 from the Singapore Government’s Research, Innovation and Enterprise 2020 plan (Advanced Manufacturing and Engineering domain); Human-Robot Interaction Phase 1 (Grant No. 192 25 00054), the National Research Foundation, Prime Minister’s Office, Singapore under the National Robotics Programme. This research is also funded by the Deutsche Forschungsgemeinschaft (DFG, German Research Foundation) under Germany’s Excellence Strategy (University Allowance, EXC 2077, University of Bremen).

Zexu Pan is with the Integrative Sciences and Engineering Programme, and the Institute of Data Science, National University of Singapore, 119077 Singapore (e-mail: pan_zexu@u.nus.edu).

Zexu Pan, Meng Ge, and Haizhou Li are with the Department of Electrical and Computer Engineering, National University of Singapore, 119077 Singapore (e-mail: gemeng@tju.edu.cn, haizhou.li@nus.edu.sg).

Meng Ge is also with the Tianjin Key Laboratory of Cognitive Computing and Application, College of Intelligence and Computing, Tianjin University, 300072 Tianjin, China

Haizhou Li is also with the Machine Listening Lab, University of Bremen, 28359 Bremen, Germany.

Traditional approaches are devoted to using signal processing technology and statistical theory to solve the *cocktail party* problem, such as non-negative matrix factorization [6], [7], factorial HMM-GMM [8], and computational auditory scene analysis [9]–[11]. They explore the idea of a spectro-temporal mask that simulates human’s attention based on harmonic and pitch analysis, which only lets pass the speaker of interest from a multi-talker speech. The prior studies have laid the foundation for recent progress.

With the advent of deep learning, we have seen that speech separation works well for highly [12]–[20] or sparsely [21]–[25] overlapped multi-talker speech. However, speech separation algorithms usually require the number of speakers in the multi-talker speech to be known in advance, which limits the scope of applications.

Speaker extraction study takes a different strategy, which is invariant to the number of speakers in the speech. It emulates human’s selective auditory attention in the *cocktail party*, and extracts only the speech for a speaker of interest, i.e., target speaker. Speaker extraction algorithms require an auxiliary reference to form the top-down attention on the target speaker [26]. A pre-recorded speech from the target speaker can serve as such an auxiliary reference [27]–[37]. A speaker extraction algorithm is expected to extract only the speech that has a similar voice signature to the pre-recorded speech.

Recent speaker extraction algorithms perform remarkably well for highly overlapped speech. However, in practice, the target-interference speaker overlapping ratio in meetings or daily conversations is around 20% [38], [39]. In such a sparsely overlapped multi-talker scenario, the speaker extraction algorithms, that are trained on highly overlapped speech, sometimes extract undesired interference speech as the output when the target speaker is quiet for a moment [40]. This is called the ‘false-extraction’ problem.

Humans perceive the world through various simultaneous sensory systems [41]. We attend to a speaker not only by reference to a registered voice signature, but also through other means such as observing the lips [42], or understanding the contextual relevance [43]. Neuroscience studies suggest that hearing is improved by observing the lips in a conversation [44], [45], leveraging on the temporal correlation between visemes and speech [46]. A viseme is a basic unit of visual speech, which corresponds to a set of phonemes for acoustic speech [47], [48]. In human listening, the visemes from a speaker of interest, i.e., target speaker, are used as the auxiliary reference to form the top-down attention.

Although visemes and phonemes do not have a one-to-one correspondence, visemes do provide a fine-grained cue

about underlying phonetic units being spoken [49]. Therefore, visemes are used in engineering solutions to speaker extraction as the auxiliary reference [50], [51]. Visemes also provide a high-level cue that discriminates between speech and non-speech [49], thus possibly alleviates the ‘false-extraction’ problem. In this paper, we advocate that visemes are more informative and robust than a pre-recorded speech to serve as the auxiliary reference for speaker extraction, especially from sparsely overlapped speech. Next, we summarize our contributions of this work.

- 1) We address a research problem, i.e. speaker extraction from sparsely overlapped speech, to deal with all multi-talker scenarios with one universal solution. This study brings speaker extraction a step closer to solving the *cocktail party* problem in real-world applications.
- 2) We propose to use visemes as the auxiliary reference to form the top-down auditory attention for speaker extraction from sparsely overlapped speech. We also propose a dual-path recurrent neural network architecture that captures global temporal dependencies with a dynamic receptive field.
- 3) We study a novel scenario-aware differentiated loss function for network training, and confirm its effectiveness through experiments on the proposed network architecture, as well as other state-of-the-art speaker extraction models.

The rest of the paper is organized as follows. In Section II, we discuss related work. In Section III, we formulate the proposed network. In Section IV, we present the experimental setup. In Section V, we report the experimental results. Finally, we conclude the study in Section VI.

II. RELATED WORK

Speaker extraction algorithm usually requires an auxiliary reference to form the top-down auditory attention on the target speaker. Either an auditory or a visual reference may serve as such auxiliary reference. Next, we discuss the prior studies for three related tasks to set the stage for our study.

A. Highly overlapped speech with audio cue

Each speaker has a unique voice signature, which can be characterized by a speaker embedding, such as i-vector [52], x-vector [53], and d-vector [54]. Given a speech sample, the speaker embedding can be derived by a speaker encoder that is trained with a speaker recognition task [55].

VoiceFilter [28] employs the d-vector encoded from a pre-recorded speech, that serves as an audio cue, to form the top-down attention for speaker extraction. The study explores the discriminative power of the d-vector to find the speech track in the multi-talker speech that has a similar voice signature as the d-vector, and extracts that speech track out.

SpEx [1] and SpEx+ [29] further the idea of speaker embedding by jointly training the speaker encoder with the speaker extractor network in a multi-task learning framework. The speaker extractor network is trained by a signal reconstruction loss while the speaker encoder is trained with a speaker recognition loss. In this way, the resulting speaker embedding

is not only discriminative between speakers, but also optimized for speaker extraction.

In most of the speaker extraction studies, it was assumed that speakers highly overlap in the multi-talker speech, and the target speaker is always present. The case of highly overlapped speech puts the speaker extraction algorithm in a stress test. However, it only represents one of many possible multi-talker scenarios. There are other scenarios, for example, the speaker of interest is not present, or the speaker of interest is the only speaker in the speech. To work in real-world applications, a speaker extraction system needs to perform across all scenarios.

B. Sparsely overlapped speech with audio cue

In natural speech communication, interlocutors typically take turns to speak, resulting in sparsely overlapped speech. In particular, a speaker of interest could be quiet throughout while some others are speaking. This scenario is referred to as sparsely overlapped speech with absent target speaker in this paper. In such a scenario, a speaker extraction algorithm trained under highly overlapped speech scenarios may fail, and produce ‘false-extraction’. Several studies try to overcome such ‘false-extraction’.

When the target speaker is absent, the commonly used scale-invariant signal-to-noise ratio (SI-SDR) [56] loss is undefined. In X-TaSNet [57], the energy of the target’s extracted speech is used as the training objective function when the target speaker is absent, while the SI-SDR loss is used when the target speaker is present.

In a recent study, *silence evaluating SI-SDR* (SE-SI-SDR) loss [40] is proposed as a unified training objective for both cases either the target speaker is absent or present. With the SE-SI-SDR loss, the SpEx+ [29] achieves the state-of-the-art performance. In another study of the VAD-SE network [58], a target speaker voice activity detection (VAD) module and a speaker extraction network [58] are jointly trained. During run-time inference, the VAD mutes the speaker extraction output when the target speaker is inactive. In other words, the speaker extraction performance highly depends on the VAD accuracy. The VAD-SE network works for multi-talker speech with absent target speaker, as well as that with present target speaker at any target-interference speaker overlapping ratios.

Both the SE-SI-SDR loss [40] and the VAD-SE [58] network overcome the ‘false-extraction’ problem in speaker extraction for sparsely overlapped speech. They all use an audio cue, i.e. a pre-recorded speech sample, as the auxiliary reference. In this paper, we explore the use of a visual cue, i.e. lips movement that doesn’t require the pre-recording of speech, instead of an audio cue for the speaker extraction task.

Furthermore, furthering the idea in X-TaSNet [57], we propose a scenario-aware differentiated loss function in this paper, to minimize the energy of an audio segment when the target speaker is quiet, and maximize the SI-SDR of an audio segment when the target speaker is speaking.

C. Highly overlapped speech with visual cue

In the *cocktail party* problem, the visual reference, if present, is not corrupted by either acoustic noise or interfer-

ence speech, which can be employed to form the top-down attention on the target speaker. The visual reference usually takes the form of a single face image from the target speaker, or a video sequence of lips of the target speaker that is synchronized with the speech.

FaceFilter [59] makes use of a single face image, and explores the general relationship between the facial appearance and the voice signature, such as age, gender, and ethnicity. The network encodes the face image into a speaker embedding to form the attention on the target speaker.

Many audio-visual speaker extraction algorithms use the visemes encoded from a sequence of lips images of the target speaker as the visual cue. The conversation [42], MuSE [60], and Time-domain speaker extraction network (TDSE) [51] are such examples, where they pre-train a visual encoder on a visual speech recognition task [61]. The visual encoder encodes a sequence of lips images, that are synchronized with the target's speech, into a sequence of lips embeddings, also known as visemes. The lips embeddings, that are time-aligned with speech frames, are then used to model the temporal synchronization and interaction between visemes and speech.

The visemes are shown effective in disentangling a target speaker from highly overlapped speech, but have not been studied for sparsely overlapped speech. In this paper, we employ the visemes to form the top-down attention on the target speaker.

III. UNIVERSAL SPEAKER EXTRACTION NETWORK WITH VISUAL CUE

A. Sparsely overlapped speech

Let $x(\tau)$ be a multi-talker speech clip, consisting of the target's speech $s(\tau)$ and interference speaker's speech $b_i(\tau)$,

$$x(\tau) = s(\tau) + \sum_{i=1}^I b_i(\tau), \quad (1)$$

where $i \in \{1, \dots, I\}$ denotes the index of interference speakers. The task of target speaker extraction aims to recover $\hat{s}(\tau)$ that is close to $s(\tau)$ from $x(\tau)$.

In natural speech communication, a target speaker may speak and pause intermittently, interspersed with the voices of interference speakers. We summarize four possible target-interference speaker pairing scenarios, namely QQ , SQ , SS , QS , in Fig. 1. An actual sparsely overlapped speech clip $x(\tau)$ could be a random combination of any of the four scenarios, where SS denotes the scenario of highly overlapped speech in many prior studies [1], [29], while QQ , SQ , and QS are not well studied yet.

B. Network architecture

We now formulate a Universal Speaker Extraction network with Visual cue, named USEV (pronounced as 'use v') network, as depicted in Fig. 2. The network is universal because it is expected to perform in all possible target-interference speaker pairing scenarios.

The USEV network has four components, 1) The speech encoder transforms the time-domain speech samples $x(\tau)$ into

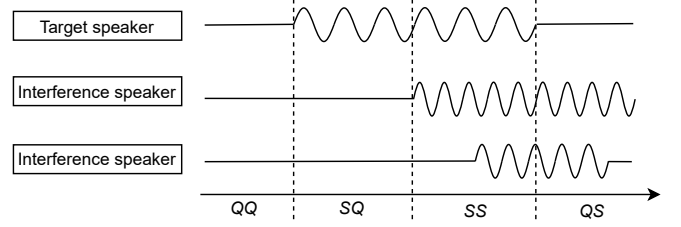


Fig. 1. An illustration of the four target-interference speaker pairing scenarios, that can happen within a sparsely overlapped speech clip. QQ : Quiet target speaker with quiet interference speaker; SQ : Speaking target speaker with quiet interference speaker; SS : Speaking target speaker with speaking interference speaker; QS : Quiet target speaker with speaking interference speaker.

a sequence of speech embeddings $X(t)$. 2) The visual encoder encodes the target's lips images into a sequence of visual embeddings $V(t)$. 3) The speaker extractor estimates a mask $M(t)$, which only lets pass the target speaker in $X(t)$. 4) The speech decoder renders the masked speech embeddings $\hat{S}(t)$ into time-domain speech samples $\hat{s}(\tau)$.

1) *Speech encoder*: We adopt the time-domain approach for the speech encoder [51] to avoid the phase estimation problem arising from the frequency-domain approach [13].

The speech encoder consists of a 1 dimensional convolution $conv1D$ followed by a rectified linear activation $relu$. The speech encoder behaves like a frequency analyzer to convert the time-domain speech samples $x(\tau)$ into a spectrum-like frame-based embedding sequence $X(t)$ in the latent space:

$$X(t) = \text{relu}(\text{conv1D}(x(\tau), 1, N, L)) \in \mathbb{R}^{N \times T} \quad (2)$$

where the $conv1D$ has input channel size 1, output channel size N , kernel size L , and stride $L/2$. The output $X(t)$ is a T frame embedding sequence of dimension of N , where $t \in \{1, \dots, T\}$.

2) *Visual encoder*: The visual encoder seeks to encode the target's lips sequence into a sequence of visual embeddings $V(t) \in \mathbb{R}^{N \times T}$, representing the target speaker's visemes, and in sync with the target's speech. We design the visual encoder with a structure similar to the visual encoder in MuSE [60], which consists of a 3 dimensional convolution $conv3D$, an 18 layer residual convolutional neural network $resnet18$, 5 repeated visual temporal convolutional network $V-TCN$, and an up-sampling layer.

The $conv3D$ and $resnet18$ are pre-trained from visual speech recognition task [61], that are denoted by a lock sign in Fig. 2. With the pre-trained weights fixed during speaker extraction training, we seek to retrain the pre-trained knowledge to encode visemes that synchronizes with the phonetic sequence of the target's speech.

The visual features extracted from the pre-trained $conv3D$ and $resnet18$ are different from the speech embeddings [62], that are not optimized for speaker extraction directly. We design an adaptation network with 5 repeated $V-TCN$ similar to the reentry model [26], with non-shared network weights, to adapt the visual embeddings towards the speaker extraction task. The architecture of a $V-TCN$ is shown in Fig. 3. The

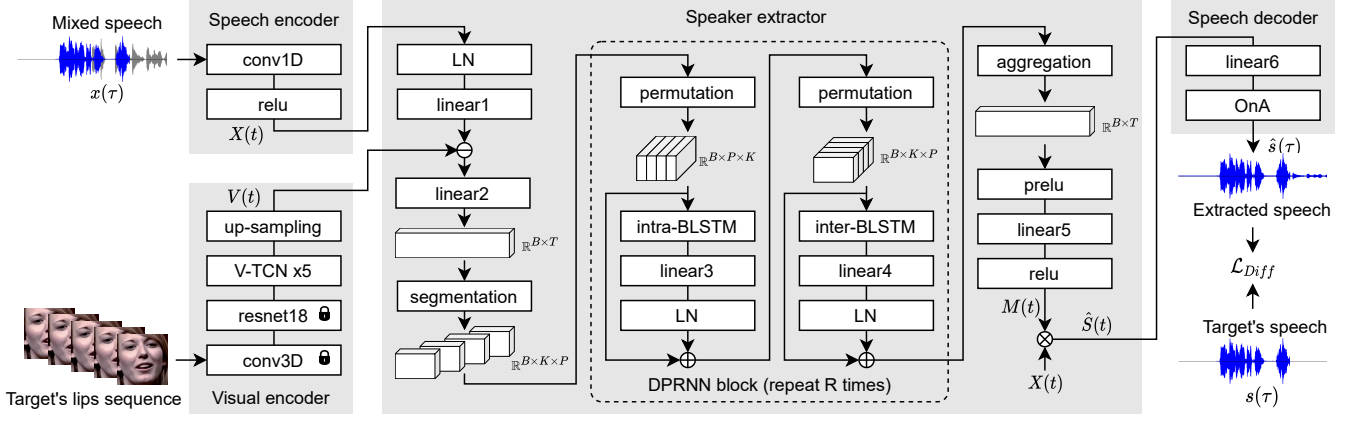


Fig. 2. The proposed universal speaker extraction network, or USEV network in short. It consists of a speech encoder, a visual encoder, a speaker extractor, and a speech decoder. The symbol \ominus refers to frame-wise concatenation of features; the symbol \oplus and \otimes refers to element-wise addition and multiplication of features. The network layers are represented by rectangles, the intermediate features are represented by 3D blocks.

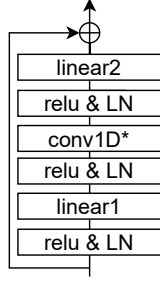


Fig. 3. The architecture of the *V-TCN* in the visual encoder. It consists of a linear layer *linear1* with input and output size N and $N * 2$ respectively; a group convolution layer *conv1D** with input channel size, output channel size, and group size $N * 2$, kernel size 3; and a linear layer *linear2* with input and output size $N * 2$ and N respectively. Each of the *linear1*, *linear2*, and *conv1D** layers are preceded with a *relu* and a layer normalization *LN*.

5 *V-TCN* is followed by an up-sampling layer to match the temporal resolution of visual embeddings to the same as the speech embeddings $X(t)$.

3) *Speaker extractor*: In computational auditory scene analysis [63], the selective filter is well studied to emulate human's selective auditory attention in attentive listening, which is usually modeled as a receptive mask. The speaker extractor in the USEV network adopts the masking method [1] to estimate a mask $M(t)$ which only lets pass the target speaker in the speech embeddings $X(t)$. The masked speech embeddings $\hat{S}(t)$ are obtained by element-wise multiplication between $X(t)$ and $M(t)$:

$$\hat{S}(t) = X(t) \otimes M(t) \in \mathbb{R}^{N \times T} \quad (3)$$

The speaker extractor requires a reference to form the top-down auditory attention on the target speaker. The visual embeddings $V(t)$ are trained just for that by providing the target speaker's visemes, that are synchronized with the target's speech. The inputs to the speaker extractor are the speech embeddings $X(t)$ and the visual embeddings $V(t)$. The studies on the *reentry* model [26], TDSE [51], and MuSE [60] suggest that, by concatenating the time-aligned visual embeddings with their corresponding speech embeddings, the speaker extractor

is able to effectively estimate the mask $M(t)$. We adopt the concatenation approach at the start of the speaker extractor.

Before the concatenation operation, $X(t)$ is passed through a layer normalization *LN*, followed by a bottleneck linear layer *linear1* [13] with input and output size N and B respectively. The concatenated embeddings are passed through a linear projection layer *linear2* with $B + N$ and B as the input and output size respectively.

In view that a speech utterance is usually encoded into a long sequence of speech embeddings. It is important to effectively model the long-term dependencies in the mask estimation process. Dilated temporal convolutional neural network (TCN) with a large receptive field has been widely used, such as WaveNet [64], Conv-TasNet [13], and TDSE [51]. However, the TCN has a fixed receptive field, thus has difficulty in learning the long-term dependencies.

DPRNN [15] is a dual-path recurrent neural network for speech separation, which has a dynamic receptive field to capture global dependencies. DPRNN segments a long sequence of embeddings into short chunks and applies intra- and inter-chunk operations with an interlacing structure. Inspired by that, we propose a dual-path structure in the context of audio-visual speaker extraction, which consists of a segmentation layer, R repeated DPRNN blocks, and an aggregation layer in the speaker extractor.

After the linear projection layer *linear2*, the 2D vector is passed through a segmentation layer, which is segmented into chunks with a window size K and hop size $K/2$. K is selected such that $K \approx \sqrt{2T}$ [15]. The resultant P chunks are concatenated to form a 3D tensor, where $P = \frac{2 \times T}{K} + 1$.

After segmentation, the 3D tensor is passed through R repeated DPRNN blocks with non-shared network weights, each with a chain of intra-chunk processing and inter-chunk processing with residual connections. The intra-chunk processing has an intra-bidirectional long short-term memory *intra-BLSTM*, with input and hidden size B and $B \times 2$ respectively, which is applied to the intra-chunk sequence (K dimension) of the 3D tensor. The *intra-BLSTM* is followed by a linear layer *linear3* with input and output size $B \times 4$ and B respectively, and a *LN*. Similar to the intra-chunk processing, the inter-

chunk has a similar network architecture and parameters, except that the *inter-BLSTM* is applied to the inter-chunk sequence (P dimension) of the $3D$ tensor.

The aggregation layer is an inverse operation of the segmentation layer, which transforms the $3D$ tensor back to $2D$. It is followed by a parametric rectified linear activation *prelu*, a linear layer *linear5* with input and output size B and N , and a *relu* layer.

4) *Speech decoder*: The speech decoder renders the masked speech embeddings $\hat{S}(t)$ into time-domain speech samples $\hat{s}(t)$. It consists of a linear layer *linear6* and an overlap-and-add operation *OnA*:

$$\hat{s}(\tau) = \text{OnA}(\text{Linear6}(\hat{S}(t), N, L), L/2) \quad (4)$$

where the *OnA* operation has a frame shift of $L/2$.

C. Scenario-aware differentiated loss

In time-domain speaker extraction algorithms, the scale-invariant signal-to-noise ratio (SI-SDR) [56] is widely used as the objective function during training. It performs very well in the case of highly overlapped speech.

However, when the target speaker is absent from the speech clip, the SI-SDR is undefined. In X-TaSNet [57], it was proposed to minimize the energy of the extracted speech, while in SE-SI-SDR [40], a stabilized version of SI-SDR was adopted as the objective function, which reduces to measuring the energy of the extracted speech with a linear transformation. They show that using the energy of the extracted speech as the training objective effectively mutes the network output when the target speaker is absent.

A sparsely overlapped speech could contain 4 target-interference speaker pairing scenarios QQ, SQ, SS, QS , as defined in Fig. 1. We propose a training strategy with a scenario-aware differentiated loss function to deal with the four scenarios during training as summarized in Fig. 4.

As we can easily obtain the target-interference speaker pairing scenario labels, we segregate the extracted speech $\hat{s}(t)$ into 4 scenario segments, i.e., QQ, SQ, SS, QS . For SQ and SS segments where the target speaker is acoustically present, we apply the SI-SDR as the loss function between the ground-truth and the extracted speech as follows,

$$\mathcal{L}_S = -10 \log_{10} \left(\frac{\| \frac{\langle \hat{s}, s \rangle}{\|\hat{s}\|^2 + \epsilon} \|^2}{\| \hat{s} - \frac{\langle \hat{s}, s \rangle}{\|\hat{s}\|^2 + \epsilon} s \|^2 + \epsilon} + \epsilon \right) \quad (5)$$

where ϵ is a small value of $1e-8$. We omit the subscript (τ) for the clean $s(\tau)$ and extracted speech segments $\hat{s}(\tau)$ in the formula for brevity.

For QQ and QS segments where the target speaker is acoustically absent, we apply the energy of the segments as the loss function,

$$\mathcal{L}_E = 10 \log_{10} (\|\hat{s}\|^2 + \epsilon) \quad (6)$$

As the loss functions of 4 scenarios may produce numerical values of different ranges, we define the total loss \mathcal{L}_{Diff} as a weighted sum of the 4 differentiated loss values as follows,

$$\mathcal{L}_{Diff} = \alpha \mathcal{L}_E^{QQ} + \beta \mathcal{L}_S^{SQ} + \gamma \mathcal{L}_S^{SS} + \delta \mathcal{L}_E^{QS} \quad (7)$$

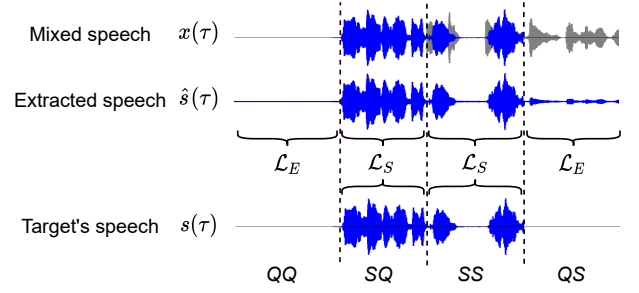


Fig. 4. An illustration of the scenario-aware differentiated loss. We segment an extracted speech clip according to the different target-interference speaker pairing scenarios (QQ, SQ, SS, QS) and apply separate loss functions for different segments.

where $\alpha, \beta, \gamma, \delta$ are the weights for the loss functions.

It is worth noting that the labels of the four scenarios are only required for training, but not during run-time inference. At run-time, a test speech clip may consist of one or more scenarios. Although we apply the scenario-aware differentiated loss to individual scenarios during training, we report the speaker extraction performance by applying a single evaluation metric, i.e., improvement on SI-SDR (SI-SDRi) or energy, over an entire speech clip.

D. Training procedure

The overall training of the USEV network consists of three stages.

- 1) The *conv3D* and *resnet18* layers in the visual encoder are pre-trained on a visual speech recognition tasks¹. The two layers are then kept frozen during subsequent training.
- 2) The entire USEV network is pre-trained on highly overlapped speech clips, with the SI-SDR loss as shown in Eq. (5). This allows the USEV network to focus on the SS scenario as it is the most difficult scenario among the four [40].
- 3) The entire USEV network is trained on sparsely overlapped speech clips, with the scenario-aware differentiated loss as shown in Eq. (7).

E. Relationship with SpEx+ and TDSE

The USEV network is a departure from the SpEx+ [29] and TDSE [51] networks. They are different mainly in the following three aspects.

- 1) The SpEx+ network represents the state-of-the-art speaker extraction algorithm that uses a pre-recorded speech as the auxiliary reference for speaker extraction, while the USEV network uses visemes as the auxiliary reference.
- 2) The SpEx+ and TDSE networks are designed for highly overlapped speech, which is neither a universal nor realistic acoustic scenario. The USEV network seeks

¹The *conv3D* and *resnet18* structures follow [65], and their pre-trained weights on visual speech recognition task are taken from https://github.com/lordmartian/deep_avsr

TABLE I

A SUMMARY OF THE NUMBER OF SPEECH CLIPS FOR DIFFERENT TARGET-INTERFERENCE SPEAKER OVERLAPPING RATIOS, AND TOTAL DURATION FOR 4 TARGET-INTERFERENCE PAIRING SCENARIOS IN THE SIMULATED IEMOCAP-MIX DATASET. CA REFERS TO THE CASE WHERE TARGET SPEAKER IS ABSENT FROM THE SPEECH CLIP.

	CA	0 %	Target-interference speaker overlapping ratio					Duration (hour)			
			(0,20] %	(20,40] %	(40,60] %	(60,80] %	(80,100] %	QQ	SQ	SS	QS
#training	20,437	34,859	24,256	46,846	73,533	84,946	115,123	48.73	83.19	266.34	133.41
#validation	295	585	496	1,112	1,869	2,129	3,514	0.85	1.79	7.53	3.01
#test	169	379	282	649	1,081	1,492	1,948	0.53	1.05	4.19	1.74

to address all possible multi-talker scenarios in *cocktail party*, which represents an important step towards real-world applications.

- 3) The speaker extractors of the SpEx+ and TDSE networks are based on the TCN [13] structure, which has a fixed receptive field in estimating the receptive mask for the target speaker. The USEV network features a DPRNN [15] structure to estimate the receptive mask, which captures global dependencies with a dynamic receptive field.

IV. EXPERIMENTAL SETUP

A. Dataset

1) *Highly overlapped speech (VoxCeleb2-mix)*: We use the VoxCeleb2 [66] dataset to create a highly overlapped speech dataset, denoted as VoxCeleb2-mix. The dataset is used for system pre-training.

The VoxCeleb2 dataset is an audio-visual dataset derived from YouTube videos. It has over 1 million videos from 6,112 celebrities. The videos are pre-processed with face detection and tracking algorithms. The resulting face tracking sequences are used as auxiliary references both for training and testing. We sample the audios at 16 kHz, the videos are synchronized with the audios and sampled at 25 FPS.

To create the VoxCeleb2-mix dataset, we randomly select 320,000 videos from 3,200 speakers in the original train set to create a training set (160,000 speech clips), and 36,237 videos from 118 speakers in the original test set to form a test set (3,000 speech clips). In either case, we only include videos that have at least 4 seconds of duration. To simulate a highly overlapped speech clip, an interference speech is mixed with the target speech at a Signal-to-Noise ratio (SNR) randomly set between 10 dB to -10 dB. Between the two mixing speech clips, the longer clip is truncated to the length of the shorter one to maximize the overlap.

2) *Sparsely overlapped speech (IEMOCAP-mix)*: We use the Interactive Emotional Dyadic Motion Capture (IEMOCAP) [67] dataset to simulate the sparsely overlapped speech clips, named IEMOCAP-mix dataset. It is used to train and evaluate the contrastive baselines and the proposed USEV network.

The IEMOCAP dataset is an acted, multi-modal dataset. It consists of 12 hours of 150 dyadic conversations, each conversation has 2 speakers, with a total of 10 speakers in the dataset. The speakers' faces are always visible throughout, either speaking or not. We sample the audios at 16 kHz, the

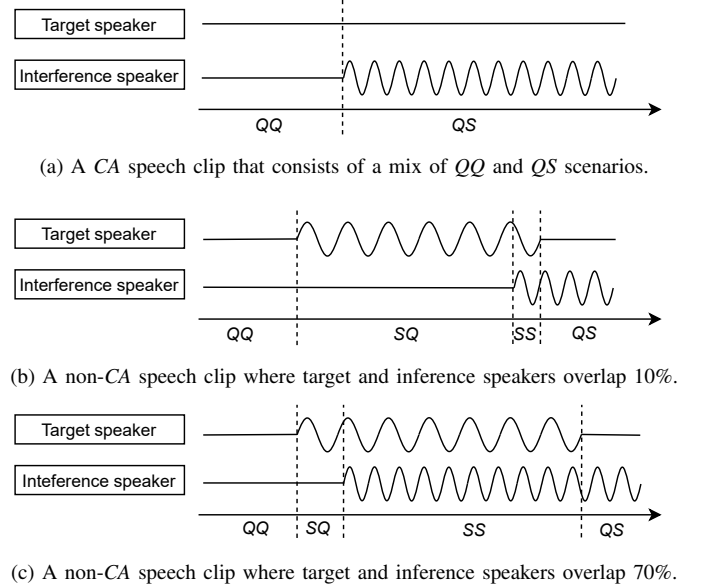


Fig. 5. Illustration of real world speech clips. (a) is a CA example. (b) and (c) are two non-CA examples.

videos are synchronized with the audios and sampled at 25 FPS.

We first obtain video clips with clean utterances from the conversations. The utterances are then used to simulate sparsely overlapped speech clips that cover all scenarios as described in Fig. 1.

From the original IEMOCAP dataset, we detect and track the faces in the videos following the VoxCeleb2 procedure [66], and obtain 300 face tracking videos. Based on the available speaker diarization label in the IEMOCAP dataset, we mute the audio when the face in the video is not speaking. In this way, each face tracking video consists of alternating quiet and speech segments, where a speech segment is always associated with the face in the video. We randomly select 240, 30, and 30 face tracking videos to simulate IEMOCAP-mix training, validation, and test sets respectively. A speaker may appear in multiple sets, but the speech does not. We split a face tracking video into multiple utterances by using a random quiet position between adjacent utterances as the delimiter.

To simulate sparsely overlapped speech clips, we drop the utterances that are shorter than 3 seconds. We use a random segment from a target speaker's utterance, and mix it with random segments from 1 or 2 interference speaker's utterances at an SNR ratio between 10 dB to -10 dB. Each speech clip

could contain speech under one or more of the four scenarios as described in Fig. 1. In this way, the dataset covers all four scenarios. We simulate 400,000, 10,000, and 6,000 speech clips for IEMOCAP-mix training, validation and test sets.

3) *Composition of IEMOCAP-mix*: As a speech clip contains speech under one or more of the four scenarios, namely *QQ*, *SQ*, *SS*, *QS*. We record the start and endpoints of the scenarios in each speech clip. With such scenario labels, the training data are ready for network training with the scenario-aware differentiated loss, while the test data can be used for reporting evaluation performance by scenarios. We report the total duration in hours for the 4 scenarios in Table I.

In addition, when the target speaker is present, we report the number of speech clips in groups by the target-interference speaker overlapping ratios, i.e., 0%, (0,20]%, (20,40]%, (40,60]%, (60,80]%, and (80,100]% in Table I. The ratio of the length of the overlapped segment to the target-interference speech segment in a speech clip is defined as the target-interference speaker overlapping ratio. When the target speaker is absent, i.e. the *CA* case, we also report the number of speech clips in Table I.

In Fig. 5, we illustrate examples of the *CA* and non-*CA* speech clips. It is worth noting that the *CA* speech clips can be in either *QQ* or *QS* scenarios, or both. But the *QQ* and *QS* scenarios can also possibly take place in the non-*CA* speech clips. To simulate real-world data, we allow multiple target-interference speaker pairing scenarios to take place in a single speech clip.

B. SE-SI-SDR loss

The SI-SDR is undefined when the target speaker is absent from the multi-talker speech. Thus, it cannot be used when we train the models on sparsely overlapped speech. The *silence evaluating SI-SDR* (SE-SI-SDR) [40] is a variant of SI-SDR, that achieves state-of-the-art performance in addressing the issue of the absent target speaker.

To compare the proposed scenario-aware differentiated loss with the SE-SI-SDR loss, we develop contrastive baselines with the SE-SI-SDR loss function for the SpEx+, TDSE, and USEV networks respectively. The SE-SI-SDR loss is formulated as follows,

$$\mathcal{L}_{SE-SI-SDR} = -20 \log_{10} \left(\frac{\| \frac{\langle \hat{s}, s \rangle s}{\|\hat{s}\|^2 + eps} \| + eps}{\| \hat{s} - \frac{\langle \hat{s}, s \rangle s}{\|\hat{s}\|^2 + eps} \| + eps} \right) \quad (8)$$

C. USEV and contrastive baselines

We select two time-domain target speaker extraction networks as the contrastive baselines, namely SpEx+ [29], [40] and TDSE [51]. The SpEx+ network employs a pre-recorded speech as the auxiliary reference, that shows the state-of-the-art performance in the presence and absence of target speaker. The TDSE network represents the recent advances of using the target's visemes as the auxiliary reference to disentangle highly overlapped speech.

1) *SpEx+*: The SpEx+ [29] network has a similar architecture with the USEV network, except that SpEx+ has a speaker encoder, which encodes the audio cue, in place of a visual encoder. In addition, the speaker extractor of SpEx+ consists of repeated stacks of TCN blocks instead of repeated DPRNN blocks in USEV. We re-implement SpEx+ by using SE-SI-SDR as the training objective [40], which is referred to as SpEx+(S). We also re-implement another variant of SpEx+ by using the scenario-aware differentiated loss as the training objective, which is referred to as SpEx+(D). Both SpEx+(S) and SpEx+(D) serve as the contrastive baselines of the USEV network.

2) *TDSE*: The TDSE [51] network has a similar architecture with the USEV network, except that the speaker extractor in TDSE consists of repeated stacks of TCN blocks instead of repeated DPRNN blocks in USEV. We re-implement TDSE by using SE-SI-SDR as the training objective, which is referred to as TDSE(S). We also re-implement another variant of TDSE by using the scenario-aware differentiated loss as the training objective, which is referred to as TDSE(D). Both TDSE(S) and TDSE(D) serve as the contrastive baselines of the USEV network.

3) *USEV*: The USEV network with the scenario-aware differentiated loss is denoted as USEV(D). We also implement a variant of the USEV network with SE-SI-SDR loss, i.e. USEV(S) for comparison.

D. Implementation details

The baselines SpEx+ and TDSE networks follow the same training procedure as the USEV network. They are pre-trained on highly overlapped speech first (VoxCeleb2-mix dataset), then trained and evaluated on the sparsely overlapped speech (IEMOCAP-mix dataset).

For pre-training on the VoxCeleb2-mix dataset, we use the adam optimizer with an initial learning rate of 0.001. The learning rate is decreased by 2% for every epoch, we train the networks for 30 epochs. During pre-training, the speech clips are truncated to 6 seconds to fit into the GPU memory.

For training on the IEMOCAP-mix dataset, we use the adam optimizer with an initial learning rate of 0.0001. The learning rate is decreased by 2% for every epoch, the training stops when the best validation loss does not improve for 8 consecutive epochs. During training, the speech clips are truncated to 6 seconds to fit into the GPU memory, during inference, the full speech clips are evaluated². The *L*, *B* and *N* are set to 40, 64 and 256 according to prior works [15], [51]. *K* is set to 100 in this paper.

V. RESULTS

We report three groups of experiments on the IEMOCAP-mix dataset. First, we empirically find the hyper-parameters and study the training procedure of the USEV network, that are reported in Section V (A). Second, we present 4 comparative studies, that are reported in Section V (B). We compare the visual cue with the audio cue in experiment 1, the

²The code is available at <https://github.com/zexupan/USEV>.

TABLE II

EXPERIMENTS OF USEV(D) WITH DIFFERENT HYPER-PARAMETERS ON THE IEMOCAP-MIX VALIDATION SET. PT MEANS THE NETWORK IS PRE-TRAINED ON THE VOXCELEB2-MIX DATASET, FT MEANS THE NETWORK IS TRAINED ON THE IEMOCAP-MIX DATASET. WE REPORT THE AVERAGE ENERGY (dB) FOR QQ AND QS SCENARIO SEGMENTS, AND SI-SDR (dB) FOR SQ AND SS SCENARIO SEGMENTS. THE LOWER THE BETTER FOR ENERGY AND THE HIGHER THE BETTER FOR SI-SDR.

System	PT	FT	R	$\alpha - \beta - \gamma - \delta$	QQ Energy	SQ SI-SDR	SS SI-SDR	QS Energy
1	✓	✓	2	0.01-0.1-1-0.01	-56.57	41.73	6.11	-27.18
2			4		-55.40	44.01	7.40	-43.35
3				0-1-1-0	-50.18	49.88	7.59	41.10
4				0-0.1-1-0	-46.85	47.03	8.00	37.13
5				0.1-1-1-0.1	-54.73	44.02	2.71	-24.60
6	✓	✓	6	0.01-1-1-0.01	-63.38	50.05	7.23	-20.53
7				0.01-0.5-1-0.01	-64.10	49.45	7.57	-32.34
8				0.01-0.3-1-0.01	-65.26	48.76	7.85	-44.16
9				0.01-0.2-1-0.01	-67.06	48.37	8.06	-53.55
10				0.01-0.1-1-0.01	-68.93	44.96	8.35	-59.03
11	✓	✗			-16.23	12.71	2.46	40.76
12	✗	✓	6	0.01-0.1-1-0.01	-79.42	34.42	3.26	-54.33

differentiated loss with the SE-SI-SDR loss in experiment 2, the DPRNN structure with the TCN structure in experiment 3. We also evaluate USEV, together with SpEx+ and TDSE under various adverse acoustic conditions in experiment 4. Third, we study how the quality of the visual cue affects the speaker extraction performance of the USEV and TDSE networks, that are reported in Section V (C).

A. Hyper-parameters and training procedure

We evaluate USEV(D) on the IEMOCAP-mix validation set to find the appropriate hyper-parameter settings and training procedures. The results are reported in Table II. To directly measure the desired results, we report the average energy of the QQ and QS scenario segments, and the average SI-SDR for the SQ and SS scenario segments. We note that the lower the better for energy, and the higher the better for SI-SDR.

We first find the best weights $\alpha, \beta, \gamma, \delta$ for the differentiated loss in the systems 3 to 10. We find that system 10 outperforms others in QQ, SS, QS scenarios with the exception that system 6 performs the best in the SQ scenario. We therefore set $\alpha, \beta, \gamma, \delta$ to be 0.01, 0.1, 1, 0.01 respectively as in system 10.

The speaker extractor in USEV(D) consists of R repeated DPRNN blocks. We study the performance of USEV(D) with different R settings. Comparing between systems 1, 2, and 10, as R increases from 2 to 6, the performance of most scenarios improves, with $R = 6$ performs the best. This is reasonable as there are more network parameters and the network is deeper as R increases. We select R to be 6 as in system 10.

USEV(D) is pre-trained on highly overlapped speech first (VoxCeleb2-mix dataset), and then trained on the sparsely overlapped speech (IEMOCAP-mix dataset). We conduct two experiments to justify this training procedure. In system 11, USEV(D) is pre-trained on the VoxCeleb2-mix dataset, but it is not trained on the IEMOCAP-mix dataset. It is seen that system 11 does not generalize as well on all target-interference speaker pairing scenarios as system 10, which is further trained on the IEMOCAP-mix dataset. This could be due to the fact that system 11 is only trained on highly overlapped speech.

In systems 1-10, USEV(D) is pre-trained on the highly overlapped VoxCeleb2-mix dataset. In system 12, we do not pre-train USEV(D) on the VoxCeleb2-mix dataset, but rather train USEV(D) directly on the IEMOCAP-mix dataset from scratch. System 12 outperforms system 10 in the QQ scenario, but lags behind system 10 in other scenarios, especially on the SS scenario in which the target's speech is highly overlapped with the interference speaker's speech. We note that SS is probably the most challenging scenario among the four, the pre-training on highly overlapped speech is effective because it well prepares the network for the SS scenario.

B. Comparative studies

As discussed in Section IV (C), SpEx+(S), TDSE(S), and USEV(S) adopt the SE-SI-SDR loss as the training objective, while SpEx+(D), TDSE(D), and USEV(D) adopt the differentiated loss as the training objective. For a fair comparison between single loss function and differentiated loss function, in both cases, we report the performance on an entire speech clip with a single evaluation metric, i.e., SI-SDRi or Energy.

In Table III, we report an overall average SI-SDRi of speech clips in the last column, and SI-SDRi by their target-interference speaker overlapping ratios. When the target speaker is absent from the speech clips which is referred to as CA , the SI-SDRi of the entire speech clip is undefined. In this case, we report the energy level of the CA speech clips.

In addition, we also report the results in terms of differentiated metrics in QQ, SQ, SS, QS scenarios in Table IV, to examine the performance over individual scenarios. The models reported in Table III and Table IV are both trained and evaluated on the IEMOCAP-mix dataset, but are evaluated using different metrics, i.e. a single SI-SDRi or energy in Table III and differentiated metrics in Table IV.

1) *Visual vs audio cue*: We compare the use of visemes with the use of a pre-recorded speech as auxiliary reference in disentangling sparsely overlapped speech on the IEMOCAP-mix test set. SpEx+(S) and SpEx+(D) employ a pre-recorded speech as the audio cue, while TDSE(S), TDSE(D), USEV(S), and USEV(D) employ the visemes as the visual cue.

TABLE III

COMPARATIVE STUDY AMONG VARIANTS OF THE SpEx+ [40], TDSE [51], AND USEV NETWORKS ON IEMOCAP-MIX TEST SET. WE REPORT THE AVERAGE ENERGY (dB) OR SI-SDRi (dB) SEPARATELY FOR TEST SAMPLES BY OVERLAPPING RATIOS. THE LOWER THE BETTER FOR ENERGY AND THE HIGHER THE BETTER FOR SI-SDRi. CA REFERS TO THE CASE WHERE THE TARGET SPEAKER IS ABSENT FROM THE SPEECH CLIP.

Model	Reference	Extractor	Loss	CA Energy	0 % SI-SDRi	(0,20] % SI-SDRi	(20,40] % SI-SDRi	(40,60] % SI-SDRi	(60,80] % SI-SDRi	(80,100] % SI-SDRi	Average SI-SDRi
SpEx+(S)	Speech	TCN	SE-SI-SDR	15.75	-16.09	9.09	5.72	5.63	5.03	4.81	2.37
SpEx+(D)			Differentiated	84.63	-9.62	9.81	8.19	6.96	6.26	6.09	4.62
TDSE(S)	Visual	TCN	SE-SI-SDR	-64.99	11.79	17.08	10.40	10.29	8.71	8.50	11.13
TDSE(D)			Differentiated	-30.79	9.62	17.72	12.15	10.68	9.56	9.19	11.49
USEV(S)	Visual	DPRNN	SE-SI-SDR	-75.23	12.75	17.00	9.22	9.38	7.99	7.75	10.68
USEV(D)			Differentiated	-65.8	12.87	18.31	12.58	10.77	9.73	9.53	12.30

TABLE IV

COMPARATIVE STUDY AMONG VARIANTS OF THE SpEx+ [40], TDSE [51], AND USEV NETWORKS ON IEMOCAP-MIX TEST SET. WE REPORT THE AVERAGE ENERGY (dB) FOR QQ AND QS SCENARIO SEGMENTS, AND SI-SDR (dB) FOR SQ AND SS SCENARIO SEGMENTS. THE LOWER THE BETTER FOR ENERGY AND THE HIGHER THE BETTER FOR SI-SDR. THE NUMBERS OF NETWORK PARAMETERS (PARAM) ARE REPORTED IN MILLION (M).

Model	Reference	Extractor	Loss	QQ Energy	SQ SI-SDR	SS SI-SDR	QS Energy	Param (M)
SpEx+(S)	Speech	TCN	SE-SI-SDR	-13.77	16.15	2.81	17.66	11.9
SpEx+(D)			Differentiated	4.72	32.01	4.94	68.27	
TDSE(S)	Visual	TCN	SE-SI-SDR	-20.17	32.64	6.47	32.62	22.1
TDSE(D)			Differentiated	-32.80	45.47	7.54	-26.78	
USEV(S)	Visual	DPRNN	SE-SI-SDR	-53.07	31.00	5.65	-12.30	15.3
USEV(D)			Differentiated	-67.71	44.76	7.68	-57.51	

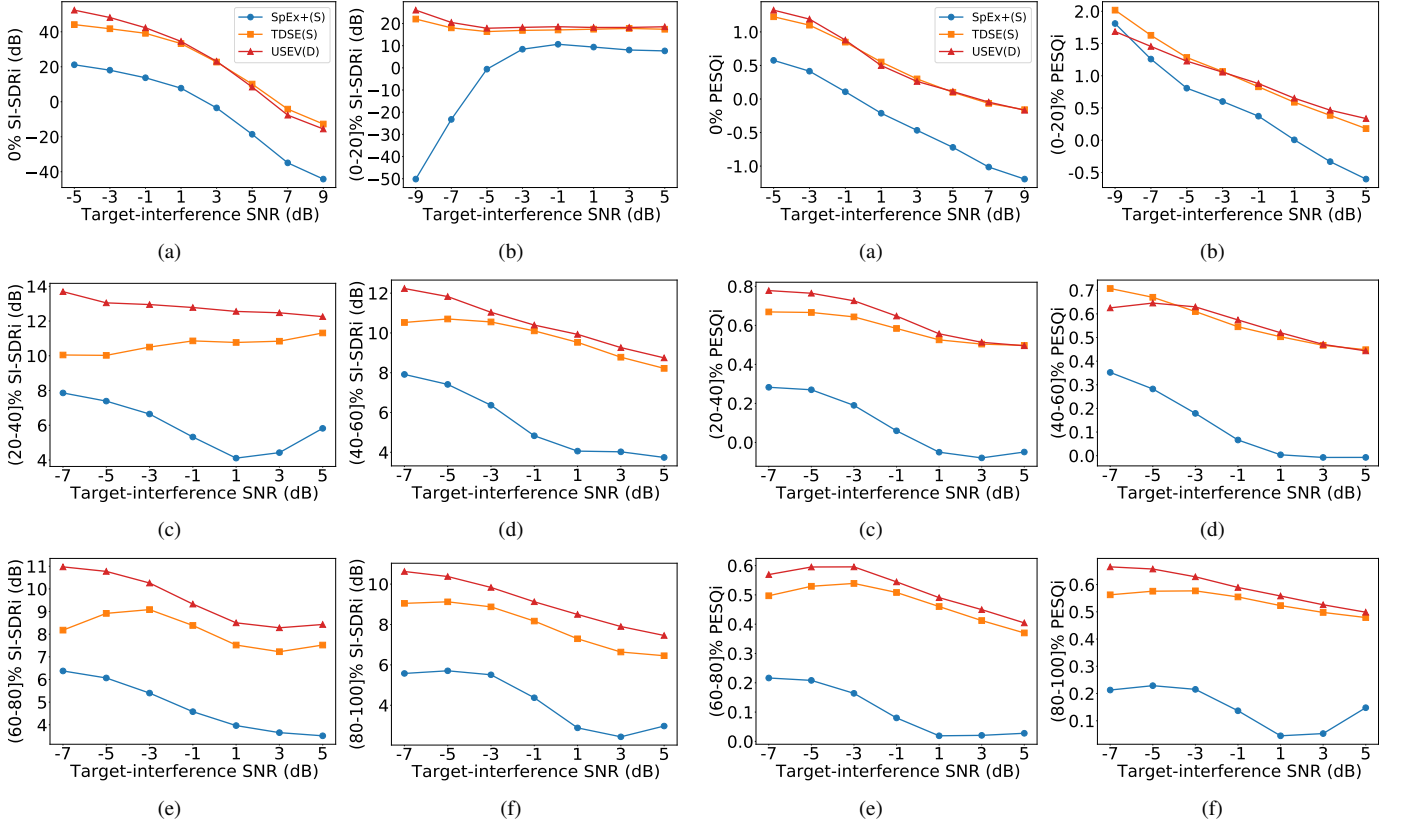


Fig. 6. The average SI-SDRi by SpEx+(S), TDSE(S), and USEV(D) on the IEMOCAP-mix dataset as a function of the target-interference SNR. We plot the results for 6 target-interference speaker overlapping ratios separately in figures (a) to (f).

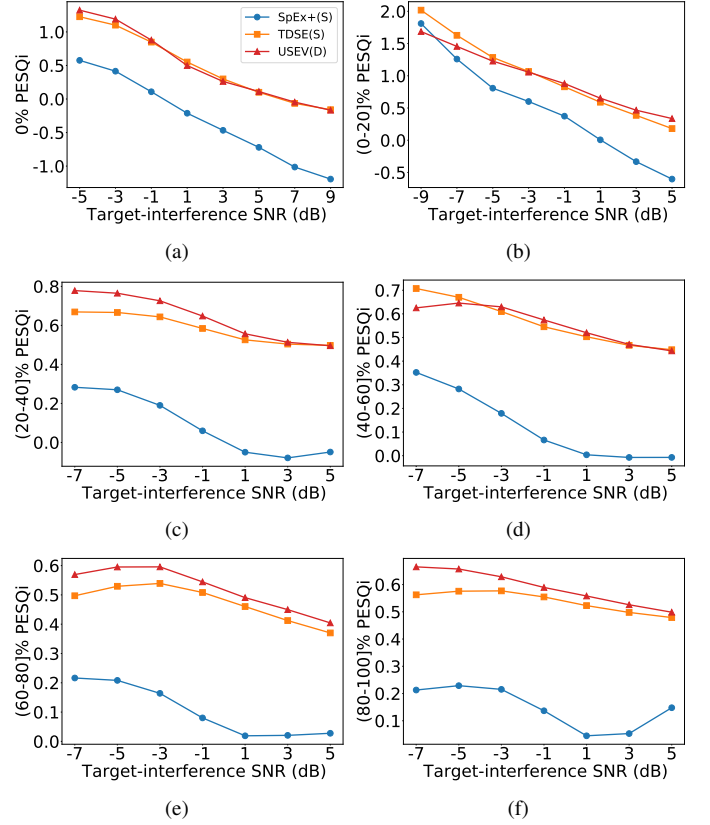


Fig. 7. The average PESQi by SpEx+(S), TDSE(S), and USEV(D) on the IEMOCAP-mix dataset as a function of the target-interference SNR. We plot the results for 6 target-interference speaker overlapping ratios separately in figures (a) to (f).

SpEx+(S), TDSE(S), and USEV(S) are trained using the SE-SI-SDR loss. As shown in Table III, TDSE(S) and USEV(S) consistently outperform SpEx+(S). As shown in Table IV, TDSE(S) outperforms SpEx+(S) in all scenarios except for *QS*. USEV(S) outperforms SpEx+(S) in all scenarios. Results show that when the SE-SI-SDR loss is used, the visemes outperform the pre-recorded speech.

SpEx+(D), TDSE(D), and USEV(D) are trained using the differentiated loss. The weights of the differentiated loss are selected the same as system 10 in Table II. As shown in Table III, TDSE(D) and USEV(D) consistently outperform SpEx+(D) on all overlapping ratios. As shown in Table IV, USEV(D) and TDSE(D) consistently outperform SpEx+(D) in all scenarios. Results show that when the differentiated loss is used, the visemes outperform the pre-recorded speech.

As shown in Table IV, SpEx+(S) and SpEx+(D) both have high energy in *QS* scenarios, which means that the networks have undesired output when the target speaker is quiet, experiencing the ‘false-extraction’. Among the audio-visual implementations, TDSE(D), USEV(S), and USEV(D) have low energy in *QS* scenarios, except for TDSE(S). Overall experimental results show that the visual cue outperform a pre-recorded speech in disentangling sparsely overlapped speech.

2) *Differentiated loss vs SE-SI-SDR loss*: We compare the use of differentiated loss with the SE-SI-SDR loss on the baselines and our proposed USEV network in disentangling sparsely overlapped speech from the IEMOCAP-mix test set.

As shown in Table III, SpEx+(D) outperforms SpEx+(S) on all overlapping ratios except for *CA* cases. As shown in Table IV, SpEx+(D) performs better in *SQ* and *SS* scenario, but SpEx+(S) performs better in *QQ* and *QS* scenario. For the SpEx+ network, the SE-SI-SDR loss focuses more on the segments in which the target speaker is quiet, while the differentiated loss focuses more on the segments in which the target speaker is speaking.

As shown in Table III, TDSE(D) outperforms TDSE(S) on all overlapping ratios except for the 0% and *CA* cases. As shown in Table IV, TDSE(D) outperforms TDSE(S) in all scenarios. The differentiated loss performs better than the SE-SI-SDR loss on the TDSE network.

As shown in Table III, USEV(D) outperforms USEV(S) on all overlapping ratios except for the *CA* case. As shown in Table IV, USEV(D) outperforms USEV(S) in all scenarios. Our proposed USEV(D) trained with the differentiated loss is best suited for sparsely overlapped speaker extraction compared with the TDSE and SpEx+ networks.

3) *DPRNN vs TCN*: We compare the effectiveness of DPRNN with TCN in the speaker extractor when the visual cue is employed as the auxiliary reference. The TDSE network employs a repeated stack of TCN in the speaker extractor to estimate the receptive mask, while the USEV network employs a repeated DPRNN block to estimate the receptive mask.

As shown in Table III, when the SE-SI-SDR loss is used to for network training, USEV(S) performs better than TDSE(S) in *CA* and 0% cases, but TDSE(S) performs better on other overlapping ratios. As shown in Table IV, USEV(S) performs better in *QQ* and *QS* scenario, but TDSE(S) performs better in *SQ* and *SS* scenario. This shows that when the SE-SI-

SDR loss is used, the TCN structure performs better on the segments in which the target speaker is speaking, while the DPRNN structure performs better on the segments in which the target speaker is quiet.

As shown in Table III, when the differentiated loss is used to for network training, USEV(D) outperforms TDSE(D) on all overlapping ratios. As shown in Table IV, USEV(D) outperforms TDSE(D) in all scenarios, except for the *SQ* scenario. This shows that only when the proposed differentiated loss is used, the DPRNN outperforms the TCN structure. Overall, USEV(D) achieves the best performance on the IEMOCAP-mix test set.

4) *Effect of target-interference speaker overlapping ratio and SNR*: To evaluate how the speaker extraction networks perform in adverse acoustic conditions, we first group the test data according to the extent to which the speakers overlap. At each target-interference speaker overlapping ratio, we report the performance for speech clips with different levels of energy contrast between the target speaker and the interference speaker in terms of signal-to-noise ratio (SNR), where signal refers to the target, while noise refers to the interference.

In Fig. 6, the speech clips are first grouped into 6 categories according to their target-interference speaker overlapping ratio, and are separately plotted in subplot (a) to (f). At each overlapping ratio, we plot the SI-SDR_i gain against different target-interference SNR. Similarly, in Fig. 7, we plot the improvement on perceptual evaluation of speech quality (PESQ_i) gain against different target-interference SNR, at each target-interference speaker overlapping ratio.

It is observed that USEV(D) consistently outperforms SpEx+(S) and TDSE(S) in terms of SI-SDR_i and PESQ_i for all target-interference speaker overlapping ratios and across various target-interference SNR. As SNR increases, the SI-SDR_i and PESQ_i gain reduce.

5) *Model size*: We also compare the model sizes of the SpEx+, TDSE, and USEV networks in Table IV. The TDSE and USEV network have more network parameters compared with the SpEx+ network due to the large visual encoder module. The USEV network has 6.8 million fewer parameters compared with the TDSE network due to the smaller size of the DPRNN blocks. The no. of network parameters reported for the TDSE and USEV network do not include the face detection and tracking module.

C. Effect of the quality of visual cue

When using visual cue to form a top-down auditory attention, the quality of visual cue matters. Next, we study two situations where the quality of the visual cue is compromised by evaluating the USEV and TDSE networks.

1) *Visual occlusion*: When face detection and tracking algorithms fail to detect the target speaker, or the lips are occluded for some reason, the visual cue is absent or incomplete. We simulate the above scenario, referred to as visual occlusion, by blacking out a random segment of the visual reference for each speech clip in the IEMOCAP-mix dataset, while keeping the audio signal intact. We study the impact of such visual occlusion on the audio-visual models, namely

TABLE V

COMPARATIVE STUDY AMONG VARIANTS OF THE TDSE [51], AND USEV NETWORKS ON IEMOCAP-MIX TEST SET FOR VISUAL CUE WITH OCCLUSION. THE AVERAGE ENERGY (dB) OR SI-SDRi (dB) ARE REPORTED FOR MODELS THAT ARE TRAINED ON IEMOCAP-MIX TRAINING DATA WITH AND WITHOUT OCCLUSION (OCCL.). THE LOWER THE BETTER FOR ENERGY AND THE HIGHER THE BETTER FOR SI-SDRi.

Model	Extractor	Loss	Train Occl.	CA Energy	0 % SI-SDRi	(0,20] % SI-SDRi	(20,40] % SI-SDRi	(40,60] % SI-SDRi	(60,80] % SI-SDRi	(80,100] % SI-SDRi	Average SI-SDRi
TDSE(S)	TCN	SE-SI-SDR	✗	-71.67	-35.13	-4.11	-15.03	-17.59	-15.16	-10.23	-16.21
TDSE(D)	TCN	Differentiated		-16.41	-25.52	5.06	-0.40	-3.44	-3.31	-1.71	-4.89
USEV(S)	DPRNN	SE-SI-SDR		-74.20	-25.28	-1.01	-15.58	-20.81	-16.67	-12.84	-15.37
USEV(D)	DPRNN	Differentiated		-62.82	-25.71	-0.27	-6.37	-11.10	-10.82	-5.99	-10.04
TDSE(S)	TCN	SE-SI-SDR	✓	-57.80	9.54	15.88	7.83	8.11	6.94	7.21	9.25
TDSE(D)	TCN	Differentiated		15.95	10.32	16.42	11.86	10.26	9.27	8.66	11.13
USEV(S)	DPRNN	SE-SI-SDR		-64.85	11.02	15.46	7.54	6.16	4.66	5.31	8.36
USEV(D)	DPRNN	Differentiated		-31.38	14.15	16.12	11.67	9.48	8.87	8.10	11.40

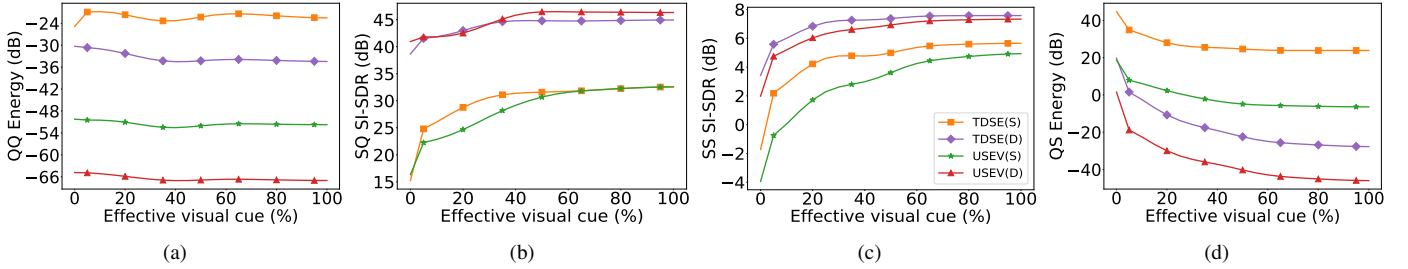


Fig. 8. Comparative study among TDSE(S), TDSE(D), USEV(S), and USEV(D) with partially occluded visual reference. The models are trained on the IEMOCAP-mix training data with visual occlusion. We report the performance in QQ , SQ , SS , QS scenarios separately as a function of the effective visual cue, i.e. the ratio of the effective visual duration to the total length of speech clip. The lower the better for energy in (a) QQ scenario and (d) QS scenario, and the higher the better for SI-SDR in (b) SQ scenario and (c) SS scenario.

TABLE VI

COMPARATIVE STUDIES AMONG VARIANTS OF THE TDSE [51], AND USEV NETWORKS ON IEMOCAP-MIX TEST SET FOR OUT-OF-SYNC VISUAL CUE. THE AVERAGE ENERGY (dB) OR SI-SDRi (dB) ARE REPORTED FOR MODELS THAT TRAINED WITH AND WITHOUT OUT-OF-SYNC (OS.) DATA. THE LOWER THE BETTER FOR ENERGY AND THE HIGHER THE BETTER FOR SI-SDRi.

Model	Extractor	Loss	Train OS.	CA Energy	0 % SI-SDRi	(0,20] % SI-SDRi	(20,40] % SI-SDRi	(40,60] % SI-SDRi	(60,80] % SI-SDRi	(80,100] % SI-SDRi	Average SI-SDRi
TDSE(S)	TCN	SE-SI-SDR	✗	-53.81	-6.53	9.13	2.09	3.28	3.86	2.75	2.43
TDSE(D)	TCN	Differentiated		-17.55	-3.00	12.93	6.91	6.20	5.80	4.96	5.63
USEV(S)	DPRNN	SE-SI-SDR		-74.31	-21.01	0.54	-8.01	-4.10	-1.92	-3.27	-6.30
USEV(D)	DPRNN	Differentiated		-63.80	-18.78	6.64	0.73	0.54	2.43	1.99	-1.08
TDSE(S)	TCN	SE-SI-SDR	✓	-67.05	10.60	17.85	11.01	10.09	8.88	8.38	11.14
TDSE(D)	TCN	Differentiated		13.63	8.36	17.83	12.30	10.83	9.70	8.91	11.32
USEV(S)	DPRNN	SE-SI-SDR		-68.96	9.01	16.37	8.75	8.02	6.63	6.43	9.20
USEV(D)	DPRNN	Differentiated		-35.91	13.77	17.09	12.21	10.31	9.12	8.47	11.83

TDSE(S), TDSE(D), USEV(S), and USEV(D), and present their results in Table V.

The models are first pre-trained on the VoxCeleb2-mix dataset, where there is no occlusion in the training data. In the training stage with the IEMOCAP-mix dataset, if the occlusion data are not involved (Train Occl. ✗), none of the models perform well on occlusion evaluations. If the occlusion data are involved in the training stage on the IEMOCAP-mix dataset (Train Occl. ✓), all models improve. TDSE(D) performs the best on all overlapping ratios except for the 0%, and the CA case. USEV(D) achieves comparable results with TDSE(D), but outperforms the latter by a large margin on the CA and 0% cases.

We also evaluate the models with the different effective visual cue and report the results in Fig. 8 for the four scenarios. We define the effective visual cue (%) as the ratio of the

effective visual duration to the total length of the speech clip. It is observed that USEV(D) outperforms all other models, except TDSE(D) in the SS scenario. It is seen that USEV(D) outperforms USEV(S), and TDSE(D) outperforms TDSE(S) on all scenario segments for the various effective visual cues, which shows that the differentiated loss outperforms the SE-SI-SDR loss in face of visual occlusions.

From Fig. 8, the performance of all 4 scenarios improves as the effective visual duration increases. When the effective visual cue reaches 20%, USEV(D) performs reasonably well across all scenarios. When it goes beyond 50%, USEV(D)'s performance starts to saturate.

2) *Out-of-sync visual cue*: When visual and audio are recorded using separate devices, two signals may not be synchronized, we refer to it as out-of-sync visual cue. Such out-of-sync visual cue may adversely impact the speaker extraction

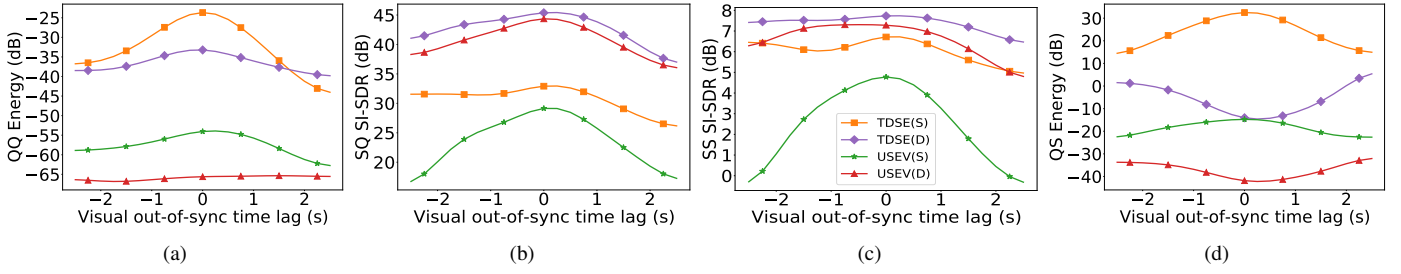


Fig. 9. Comparative study among TDSE(S), TDSE(D), USEV(S), and USEV(D) with out-of-sync visual cue. The models are trained on the IEMOCAP-mix training data with visual occlusion. We report the performance in QQ , SQ , SS , QS scenarios separately as a function of visual out-of-sync time lag. The lower the better for energy in (a) QQ scenario and (d) QS scenarios, and the higher the better for SI-SDR in (b) SQ scenario and (c) SS scenarios.

performance. We create such an out-of-sync dataset based on the IEMOCAP-mix dataset, where the visual reference is randomly shifted for a time lag of -2 to 2 seconds. We evaluate TDSE(S), TDSE(D), USEV(S), and USEV(D) to observe how they perform with such visual reference, as reported in Table VI.

The models are first pre-trained on the VoxCeleb2-mix dataset, where audio and visual are synchronized. In the training stage with the IEMOCAP-mix dataset, if the out-of-sync data are not involved in the training stage (Train OS. ✗), none of the models performs well on the out-of-sync evaluation data except for TDSE(D). If the out-of-sync data are involved in the training stage on the IEMOCAP-mix dataset (Train OS. ✓), all models improve. TDSE(D) performs the best across all overlapping ratios except for the 0%, (0, 20]% and CA cases. USEV(D) achieves comparable results with TDSE(D), but outperforms TDSE(D) by a large margin for the 0% and CA case.

In Fig. 9, we report the performance under the QQ , SQ , SS , QS scenarios in separate plots, and as a function of the out-of-sync time lag. It is observed that USEV(D) outperforms USEV(S), and TDSE(D) outperforms TDSE(S) across all scenarios, and for various out-of-sync time lags, which suggests that the differentiated loss outperforms the SE-SI-SDR loss with the out-of-sync visual cue. In addition, in the SQ , SS , QS scenarios, the USEV(D) achieves the best performance when the visual out-of-sync time lag is 0, reaffirming the contributions of the synchronized visual reference to the speaker extraction task.

VI. CONCLUSION

We propose a universal speaker extraction network with visual cue to disentangling sparsely overlapped speech for all multi-talker scenarios. The experiments show that the proposed differentiated loss function is effective, the proposed USEV network outperforms the state-of-the-art audio-visual speaker extraction techniques. The performance gain is attributed to the scenario-aware differentiated loss function, and the superiority of DPRNN over TCN extractor. This paper marks an important step towards solving a realistic *cocktail party* problem.

REFERENCES

- [1] C. Xu, W. Rao, E. S. Chng, and H. Li, “Spex: Multi-scale time domain speaker extraction network,” *IEEE/ACM Trans. Audio, Speech, Lang. Process.*, vol. 28, pp. 1370–1384, 2020.
- [2] A. W. Bronckhorst, “The cocktail party phenomenon: A review of research on speech intelligibility in multiple-talker conditions,” *Acta Acustica united with Acustica*, vol. 86, no. 1, pp. 117–128, 2000.
- [3] D. Wang, “Deep learning reinvents the hearing aid,” *IEEE spectrum*, vol. 54, no. 3, pp. 32–37, 2017.
- [4] R. Tao, R. K. Das, and H. Li, “Audio-visual speaker recognition with a cross-modal discriminative network,” in *Proc. INTERSPEECH*, 2020, pp. 2242–2246.
- [5] X. Zhou, G. Lee, E. Yilmaz, Y. Long, J. Liang, and H. Li, “Self-and-mixed attention decoder with deep acoustic structure for transformer-based lvcst,” in *Proc. INTERSPEECH*, 2020, pp. 5016–5020.
- [6] M. N. Schmidt and R. K. Olsson, “Single-channel speech separation using sparse non-negative matrix factorization,” in *Ninth International Conference on Spoken Language Processing*, 2006.
- [7] A. Cichocki, R. Zdunek, and S.-i. Amari, “New algorithms for non-negative matrix factorization in applications to blind source separation,” in *Proc. IEEE Int. Conf. Acoust., Speech, Signal Process.*, vol. 5, 2006, pp. V–V.
- [8] M. Stark, M. Wohlmayr, and F. Pernkopf, “Source-filter-based single-channel speech separation using pitch information,” *IEEE/ACM Trans. Audio, Speech, Lang. Process.*, vol. 19, no. 2, pp. 242–255, 2010.
- [9] R. Lyon, “A computational model of binaural localization and separation,” in *Proc. IEEE Int. Conf. Acoust., Speech, Signal Process.*, vol. 8, 1983, pp. 1148–1151.
- [10] D. Wang and G. J. Brown, *Computational auditory scene analysis: Principles, algorithms, and applications*. Wiley-IEEE press, 2006.
- [11] G. Hu and D. Wang, “Auditory segmentation based on onset and offset analysis,” *IEEE/ACM Trans. Audio, Speech, Lang. Process.*, vol. 15, no. 2, pp. 396–405, 2007.
- [12] J. R. Hershey, Z. Chen, J. Le Roux, and S. Watanabe, “Deep clustering: Discriminative embeddings for segmentation and separation,” in *Proc. IEEE Int. Conf. Acoust., Speech, Signal Process.*, 2016, pp. 31–35.
- [13] Y. Luo and N. Mesgarani, “Conv-tasnet: Surpassing ideal time-frequency magnitude masking for speech separation,” *IEEE/ACM Trans. Audio, Speech, Lang. Process.*, vol. 27, no. 8, pp. 1256–1266, 2019.
- [14] C. Xu, W. Rao, X. Xiao, E. S. Chng, and H. Li, “Single channel speech separation with constrained utterance level permutation invariant training using grid lstm,” in *Proc. IEEE Int. Conf. Acoust., Speech, Signal Process.*, 2018, pp. 6–10.
- [15] Y. Luo, Z. Chen, and T. Yoshioka, “Dual-path rnn: Efficient long sequence modeling for time-domain single-channel speech separation,” in *Proc. IEEE Int. Conf. Acoust., Speech, Signal Process.*, 2020, pp. 46–50.
- [16] Z. Chen, Y. Luo, and N. Mesgarani, “Deep attractor network for single-microphone speaker separation,” in *Proc. IEEE Int. Conf. Acoust., Speech, Signal Process.*, 2017, pp. 246–250.
- [17] N. Zeghidour and D. Grangier, “Wavesplit: End-to-end speech separation by speaker clustering,” *arXiv preprint arXiv:2002.08933*, 2020.
- [18] D. Stoller, S. Ewert, and S. Dixon, “Wave-u-net: A multi-scale neural network for end-to-end audio source separation,” in *Proceedings of 19th International Society for Music Information Retrieval Conference*, 2018.
- [19] M. Kolbæk, D. Yu, Z.-H. Tan, and J. Jensen, “Multitalker speech separation with utterance-level permutation invariant training of deep recurrent neural networks,” *IEEE/ACM Trans. Audio, Speech, Lang. Process.*, vol. 25, no. 10, pp. 1901–1913, 2017.
- [20] Y. Liu and D. Wang, “Divide and conquer: A deep casa approach

- to talker-independent monaural speaker separation,” *IEEE/ACM Trans. Audio, Speech, Lang. Process.*, vol. 27, no. 12, pp. 2092–2102, 2019.
- [21] C. Li, Z. Chen, Y. Luo, C. Han, T. Zhou, K. Kinoshita, M. Delcroix, S. Watanabe, and Y. Qian, “Dual-path modeling for long recording speech separation in meetings,” in *Proc. IEEE Int. Conf. Acoust., Speech, Signal Process.*, 2021, pp. 5739–5743.
 - [22] Z. Chen, T. Yoshioka, L. Lu, T. Zhou, Z. Meng, Y. Luo, J. Wu, X. Xiao, and J. Li, “Continuous speech separation: dataset and analysis,” in *Proc. IEEE Int. Conf. Acoust., Speech, Signal Process.*, 2020, pp. 7284–7288.
 - [23] T. Yoshioka, H. Erdogan, Z. Chen, and F. Alleva, “Multi-microphone neural speech separation for far-field multi-talker speech recognition,” in *Proc. IEEE Int. Conf. Acoust., Speech, Signal Process.*, 2018, pp. 5739–5743.
 - [24] S. Chen, Y. Wu, Z. Chen, J. Wu, J. Li, T. Yoshioka, C. Wang, S. Liu, and M. Zhou, “Continuous speech separation with conformer,” in *Proc. IEEE Int. Conf. Acoust., Speech, Signal Process.*, 2021, pp. 5749–5753.
 - [25] Z.-Q. Wang and D. Wang, “Count and separate: Incorporating speaker counting for continuous speaker separation,” in *Proc. IEEE Int. Conf. Acoust., Speech, Signal Process.*, 2021, pp. 11–15.
 - [26] Z. Pan, R. Tao, C. Xu, and H. Li, “Selective hearing through lip-reading,” *arXiv preprint arXiv:2106.07150*, 2021.
 - [27] K. Žmolíková, M. Delcroix, K. Kinoshita, T. Ochiai, T. Nakatani, L. Burget, and J. Černocký, “Speakerbeam: Speaker aware neural network for target speaker extraction in speech mixtures,” *IEEE Journal of Selected Topics in Signal Processing*, vol. 13, no. 4, pp. 800–814, 2019.
 - [28] Q. Wang, H. Muckenhirn, K. Wilson, P. Sridhar, Z. Wu, J. R. Hershey, R. A. Saurous, R. J. Weiss, Y. Jia, and I. L. Moreno, “VoiceFilter: Targeted Voice Separation by Speaker-Conditioned Spectrogram Masking,” in *Proc. INTERSPEECH*, 2019, pp. 2728–2732.
 - [29] M. Ge, C. Xu, L. Wang, E. S. Chng, J. Dang, and H. Li, “SpEx+: A Complete Time Domain Speaker Extraction Network,” in *Proc. INTERSPEECH*, 2020, pp. 1406–1410.
 - [30] —, “Multi-stage speaker extraction with utterance and frame-level reference signals,” in *Proc. IEEE Int. Conf. Acoust., Speech, Signal Process.*, 2021, pp. 6109–6113.
 - [31] S. He, H. Li, and X. Zhang, “Speakerfilter: Deep learning-based target speaker extraction using anchor speech,” in *Proc. IEEE Int. Conf. Acoust., Speech, Signal Process.*, 2020, pp. 376–380.
 - [32] M. Delcroix, K. Zmolikova, K. Kinoshita, A. Ogawa, and T. Nakatani, “Single channel target speaker extraction and recognition with speaker beam,” in *Proc. IEEE Int. Conf. Acoust., Speech, Signal Process.*, 2018, pp. 5554–5558.
 - [33] X. Xiao, Z. Chen, T. Yoshioka, H. Erdogan, C. Liu, D. Dimitriadis, J. Droppo, and Y. Gong, “Single-channel speech extraction using speaker inventory and attention network,” in *Proc. IEEE Int. Conf. Acoust., Speech, Signal Process.*, 2019, pp. 86–90.
 - [34] J. Shi, J. Xu, Y. Fujita, S. Watanabe, and B. Xu, “Speaker-Conditional Chain Model for Speech Separation and Extraction,” in *Proc. INTERSPEECH*, 2020, pp. 2707–2711.
 - [35] M. Delcroix, T. Ochiai, K. Zmolikova, K. Kinoshita, N. Tawara, T. Nakatani, and S. Araki, “Improving speaker discrimination of target speech extraction with time-domain speakerbeam,” in *Proc. IEEE Int. Conf. Acoust., Speech, Signal Process.*, 2020, pp. 691–695.
 - [36] H. Sato, T. Ochiai, K. Kinoshita, M. Delcroix, T. Nakatani, and S. Araki, “Multimodal attention fusion for target speaker extraction,” in *IEEE Spoken Language Technology Workshop*, 2021, pp. 778–784.
 - [37] T. Ochiai, M. Delcroix, K. Kinoshita, A. Ogawa, and T. Nakatani, “Multimodal SpeakerBeam: Single Channel Target Speech Extraction with Audio-Visual Speaker Clues,” in *Proc. INTERSPEECH*, 2019, pp. 2718–2722.
 - [38] Ö. Çetin and E. Shriberg, “Analysis of overlaps in meetings by dialog factors, hot spots, speakers, and collection site: Insights for automatic speech recognition,” in *Ninth international conference on spoken language processing*, 2006.
 - [39] J. Barker, S. Watanabe, E. Vincent, and J. Trmal, “The fifth chime’s speech separation and recognition challenge: Dataset, task and baselines,” in *Proc. INTERSPEECH*, 2018, pp. 1561–1565.
 - [40] M. Borsdorf, C. Xu, H. Li, and T. Schultz, “Universal speaker extraction in the presence and absence of target speakers for speech of one and two talkers,” in *Proc. INTERSPEECH*, 2021.
 - [41] L. Smith and M. Gasser, “The development of embodied cognition: Six lessons from babies,” *Artificial life*, vol. 11, no. 1-2, pp. 13–29, 2005.
 - [42] T. Afouras, J. S. Chung, and A. Zisserman, “The conversation: Deep audio-visual speech enhancement,” in *Proc. INTERSPEECH*, 2018, pp. 3244–3248.
 - [43] C. Li and Y. Qian, “Listen, Watch and Understand at the Cocktail Party: Audio-Visual-Contextual Speech Separation,” in *Proc. INTERSPEECH*, 2020, pp. 1426–1430.
 - [44] E. Z. Golumbic, G. B. Cogan, C. E. Schroeder, and D. Poeppel, “Visual input enhances selective speech envelope tracking in auditory cortex at a ‘cocktail party,’” *Journal of Neuroscience*, vol. 33, no. 4, pp. 1417–1426, 2013.
 - [45] M. J. Crosse, G. M. Di Liberto, and E. C. Lalor, “Eye can hear clearly now: inverse effectiveness in natural audiovisual speech processing relies on long-term crossmodal temporal integration,” *Journal of Neuroscience*, vol. 36, no. 38, pp. 9888–9895, 2016.
 - [46] G. M. Edelman, *Neural Darwinism: The theory of neuronal group selection*. Basic books, 1987.
 - [47] H. L. Bear and R. Harvey, “Phoneme-to-viseme mappings: the good, the bad, and the ugly,” *Speech Communication*, vol. 95, pp. 40–67, 2017.
 - [48] D. W. Massaro and J. A. Simpson, *Speech perception by ear and eye: A paradigm for psychological inquiry*. Psychology Press, 2014.
 - [49] D. Michelsanti, Z.-H. Tan, S.-X. Zhang, Y. Xu, M. Yu, D. Yu, and J. Jensen, “An overview of deep-learning-based audio-visual speech enhancement and separation,” *IEEE/ACM Trans. Audio, Speech, Lang. Process.*, 2021.
 - [50] A. Ephrat, I. Mosseri, O. Lang, T. Dekel, K. Wilson, A. Hassidim, W. T. Freeman, and M. Rubinstein, “Looking to listen at the cocktail party: a speaker-independent audio-visual model for speech separation,” *ACM Transactions on Graphics*, vol. 37, no. 4, pp. 1–11, 2018.
 - [51] J. Wu, Y. Xu, S. Zhang, L. Chen, M. Yu, L. Xie, and D. Yu, “Time domain audio visual speech separation,” in *Proc. IEEE Autom. Speech Recognit. Understanding Workshop*, 2019, pp. 667–673.
 - [52] N. Dehak, P. J. Kenny, R. Dehak, P. Dumouchel, and P. Ouellet, “Front-end factor analysis for speaker verification,” *IEEE/ACM Trans. Audio, Speech, Lang. Process.*, vol. 19, no. 4, pp. 788–798, 2010.
 - [53] D. Snyder, P. Ghahremani, D. Povey, D. Garcia-Romero, Y. Carmiel, and S. Khudanpur, “Deep neural network-based speaker embeddings for end-to-end speaker verification,” in *IEEE Spoken Language Technology Workshop*, 2016, pp. 165–170.
 - [54] L. Wan, Q. Wang, A. Papir, and I. L. Moreno, “Generalized end-to-end loss for speaker verification,” in *Proc. IEEE Int. Conf. Acoust., Speech, Signal Process.*, 2018, pp. 4879–4883.
 - [55] T. Liu, R. K. Das, M. Madhavi, S. Shen, and H. Li, “Speaker-utterance dual attention for speaker and utterance verification,” in *Proc. INTERSPEECH*, 2020, pp. 4293–4297.
 - [56] J. Le Roux, S. Wisdom, H. Erdogan, and J. R. Hershey, “SDR-half-baked or well done?” in *Proc. IEEE Int. Conf. Acoust., Speech, Signal Process.*, 2019, pp. 626–630.
 - [57] Z. Zhang, B. He, and Z. Zhang, “X-tasnet: Robust and accurate time-domain speaker extraction network,” in *Proc. INTERSPEECH*, 2020, pp. 1421–1425.
 - [58] Q. Lin, L. Yang, X. Wang, L. Xie, C. Jia, and J. Wang, “Sparsely overlapped speech training in the time domain: Joint learning of target speech separation and personal vad benefits,” *arXiv preprint arXiv:2106.14371*, 2021.
 - [59] S.-W. Chung, S. Choe, J. S. Chung, and H.-G. Kang, “FaceFilter: Audio-Visual Speech Separation Using Still Images,” in *Proc. INTERSPEECH*, 2020, pp. 3481–3485.
 - [60] Z. Pan, R. Tao, C. Xu, and H. Li, “Muse: Multi-modal target speaker extraction with visual cues,” in *Proc. IEEE Int. Conf. Acoust., Speech, Signal Process.*, 2021, pp. 6678–6682.
 - [61] T. Stafylakis and G. Tzimiropoulos, “Combining residual networks with lstms for lipreading,” in *Proc. INTERSPEECH*, 2017, pp. 3652–3656.
 - [62] Z. Pan, Z. Luo, J. Yang, and H. Li, “Multi-Modal Attention for Speech Emotion Recognition,” in *Proc. INTERSPEECH*, 2020, pp. 364–368.
 - [63] G. J. Brown and M. Cooke, “Computational auditory scene analysis,” *Computer Speech & Language*, vol. 8, no. 4, pp. 297–336, 1994.
 - [64] A. van den Oord, S. Dieleman, H. Zen, K. Simonyan, O. Vinyals, A. Graves, N. Kalchbrenner, A. Senior, and K. Kavukcuoglu, “Wavenet: A generative model for raw audio,” in *9th ISCA Speech Synthesis Workshop*, 2016, pp. 125–125.
 - [65] T. Afouras, J. S. Chung, and A. Zisserman, “Deep lip reading: A comparison of models and an online application,” in *Proc. INTERSPEECH*, 2018, pp. 3514–3518.
 - [66] J. S. Chung, A. Nagrani, and A. Zisserman, “Voxceleb2: Deep speaker recognition,” in *Proc. INTERSPEECH*, 2018, pp. 1086–1090.
 - [67] C. Busso, M. Bulut, C.-C. Lee, A. Kazemzadeh, E. Mower, S. Kim, J. N. Chang, S. Lee, and S. S. Narayanan, “IEMOCAP: Interactive emotional dyadic motion capture database,” *Language resources and evaluation*, vol. 42, no. 4, p. 335, 2008.